Optics Letters

Fast rate dual-comb spectrometer in the water-transparent 7.5–11.5 µm region

Luca Moretti,[1,2,*] Mathieu Walsh,[3] Nawaf Abualsaud,[4] Davide Gatti,[1,2] Marco Lamperti,[5] Jérome Genest,[3] Aamir Farooq,[4] and Marco Marangoni[1,2]

[1]Dipartimento di Fisica, Politecnico di Milano, Piazza Leonardo da Vinci 32, 20133 Milano, Italy
[2]Istituto di Fotonica e Nanotecnologie, CNR, Piazza Leonardo da Vinci 32, 20133 Milano, Italy
[3]Centre d'optique, photonique et laser, Université Laval, Québec, Québec G1V 0A6, Canada
[4]Physical Science and Engineering Division, King Abdullah University for Science and Technology (KAUST), Thuwal 23955, Saudi Arabia
[5]Department of Science and High Technology, University of Insubria, 22100 Como, Italy
*luca.moretti@polimi.it

Received 7 December 2023; revised 21 February 2024; accepted 23 February 2024; posted 28 February 2024; published 1 April 2024

We introduce a dual-comb spectrometer based on erbium fiber oscillators at 250 MHz that operates in the 7.5–11.5 µm spectral range over optical bandwidths up to 9 THz with a multi-kHz acquisition rate. Over an observation bandwidth of 0.8 THz, the signal-to-noise ratio per spectral point reaches 168 $Hz^{0.5}$ at an acquisition rate of 26 kHz, which allows the investigation of transient processes in the gas phase at high temporal resolution. The system also represents an attractive solution for multi-species atmospheric gas detection in open paths due to the water transparency of the spectral window, the use of thermo-electrically cooled detectors, and the out-of-loop phase correction of the interferograms.

https://doi.org/10.1364/OL.515199

Multi-species gas detection at rapid rates is highly desirable for studying transient chemically reacting systems, e.g., fuel pyrolysis, oxidation, heat release, and pollutant formation [1]. A complete picture of the reaction process, obtained by *in situ* multi-species measurements, enables understanding the fundamental chemical processes occurring therein and aids the development of predictive chemical kinetic models. Such models are crucial in the design and optimization of future energy systems [2].

Mid-infrared (MIR) dual-comb spectroscopy is a technique of choice for rapid multi-species detection because it offers the best mix of sensitivity, selectivity, and temporal resolution [3]. Contributions to sensitivity are coming from the access to the MIR region [4], where absorption features are stronger, and from a detection chain that can reach up to the shot-noise limit [5]. The selectivity, together with multi-species detection capability, originates instead from a combination of dense spectral sampling, down to the comb mode distance f_{rep} (from 0.1 to 1 GHz, typically), and ultrabroad optical bandwidths $\Delta\nu$ (up to tens of THz). The temporal resolution can be also very high, at $2\Delta\nu/f_{rep}^2$ limit set by the aliasing between different multi-heterodyne beat notes [3]. As an example, a measurement time of 10 µs can be reached with $f_{rep} = 250$ MHz by keeping the optical bandwidth below 1 THz. To further reduce the measurement time while keeping full resolution (comb-resolved spectrum), one should either increase f_{rep} or reduce the bandwidth $\Delta\nu$.

A relatively small number of MIR dual-comb spectrometers have so far been optimized from a time resolution perspective, particularly in the 7.5–11.5 µm range targeted here. Quantum-cascade-laser combs can emit high powers in this region and offer ultra-rapid acquisition times due to their very high repetition rates (up to several GHz [6]). However, they need to be tuned to resolve narrow gas features [7] because of the large spectral point spacing, while their spectral bandwidth is typically limited to 2 THz (60 cm^{-1}) per device. Electro-optic frequency combs are a versatile solution that allows bypassing phase-locking issues between the two combs [8], but their spectral bandwidth does not go beyond few wavenumbers. Moreover, their synthesis in the MIR is hampered by the very low efficiency of nonlinear optical processes in the cw regime [9]. A notable exception is the recently demonstrated dual-comb-pumped optical parametric oscillator, enabling sub-microsecond measurement times over a wide tuning range from 2.2 to 4 µm [10]. The optical bandwidth, however, remains limited to just few tens of GHz (1 cm^{-1}). Bandwidth-wise, the performance of dual-comb spectrometers based on mode-locked combs is unparalleled [3]. Their ultrafast nature and their high peak power make them also amenable to nonlinear synthesis across the entire MIR region. In the 3–5 µm spectral window, important demonstrations of coherent DCS were obtained in 2011, with bandwidths of about 1 THz around 3 µm [11], and in 2018, with bandwidths as large as 60 THz and coherent averaging up to several hours [12,13]. Recently, using intra-pulse difference frequency generation starting from amplified 1 GHz solid-state near-infrared oscillators, the full potential of DCS for transient gas spectroscopy was unlocked in the 3–5 µm region [14]. This work provided an excellent balance between the acquisition time (10 µs) and the optical bandwidth (4.5 THz, i.e., 150 cm^{-1}). At longer wavelengths, conversely, DCS has not been demonstrated so far at a rate beyond 130 Hz. In the implementations by Timmers *et al.* [15] and Kowligy *et al.* [16], limiting factors were a fairly low f_{rep} (100 MHz) and a

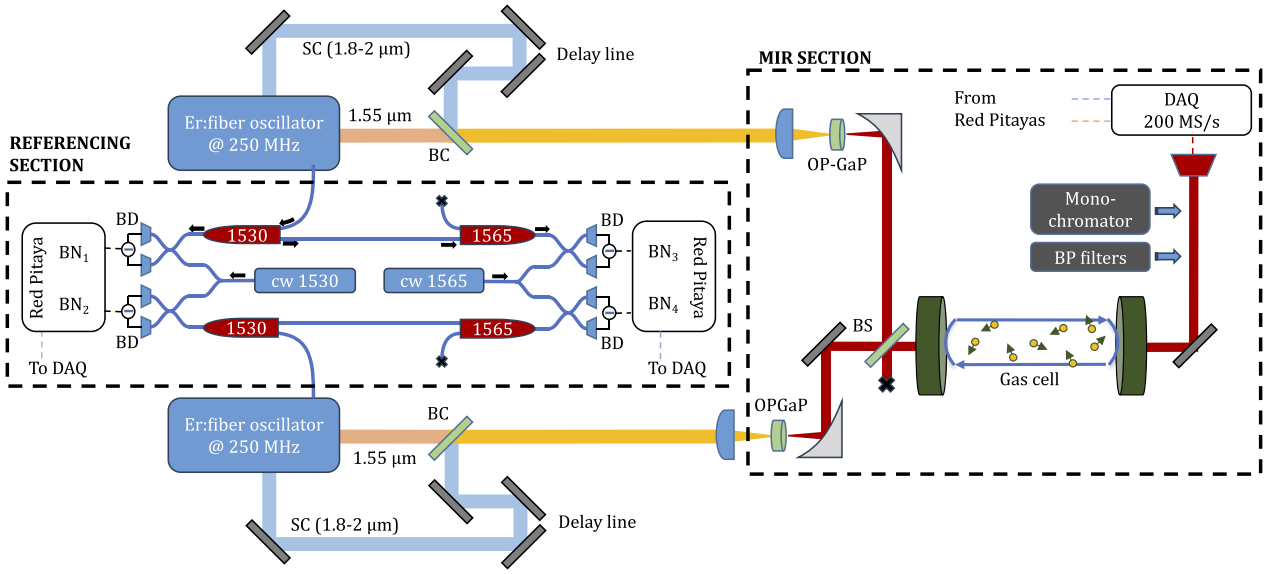

Fig. 1. Optical layout of the spectrometer based on free-space propagation for the nonlinear and spectroscopic sections and on a fiber format for the referencing section. BN, beat note; BD, balanced detector; SC, supercontinuum; BC, beam combiner; BS, beam-splitter; BP, bandpass.

small optical power (about 200 µW) combined with very large optical spectra. The power bottleneck has been drastically overcome recently, by three orders of magnitude, using amplified solid-state Cromium lasers at 2.35 µm for the MIR comb synthesis [17]. As a drawback, this is a complex and costly apparatus with a repetition frequency of only 80 MHz that is not ideal to track fast chemical dynamics.

In this work, we demonstrate comb-resolved DCS over 7.5–11.5 µm starting from two compact Erbium fiber oscillators at 250 MHz. The MIR combs are obtained by difference frequency generation (DFG) between two phase-coherent pulse trains at 1.55 and 1.85 µm. A total optical power of about 1 mW allows dual-comb spectra to be acquired up to a rate of 26 kHz over the reduced bandwidth of 0.8 THz with a figure of merit of $5 \cdot 10^5\,\mathrm{Hz}^{0.5}$ using thermo-electrically cooled detectors. Comparatively, an 80 MHz system would allow the same bandwidth to be observed at a 10 times smaller rate.

The spectrometer layout is depicted in Fig. 1 and exploits optical fibers for maximum robustness. The driving lasers are commercial Erbium fiber oscillators at 250 MHz (Menlo C-Fiber) equipped with two amplified branches, one at 1.55 µm with a power ~ 580 mW, the other coupled to a highly nonlinear fiber (HNLF) to stretch the spectrum up to 2 µm (SC branch). In the spectral region of interest for the DFG, above 1.7 µm, the signal power amounts to about 70 mW. The pulse trains from the two branches are nonlinearly mixed in an OP-GaP crystal with fan-out poling to produce broadband radiation between 8 and 12 µm. The crystal is 4 mm long, but the interaction length is about four times shorter due to a group-velocity mismatch > 100 fs/mm between the pump and signal pulses. The MIR combs interfere on a TE-cooled detector (Vigo PVI-4TE-10.6 with VPAC-1000F module), with 500 MHz bandwidth, placed downstream a gas-filled optical cell.

A monochromator or a set of bandpass filters may be introduced in the measurement branch to intentionally reduce the optical bandwidth and operate the spectrometer at a faster acquisition rate without aliasing issues. To keep the setup as simple as possible, we left the two combs free running and adopted an

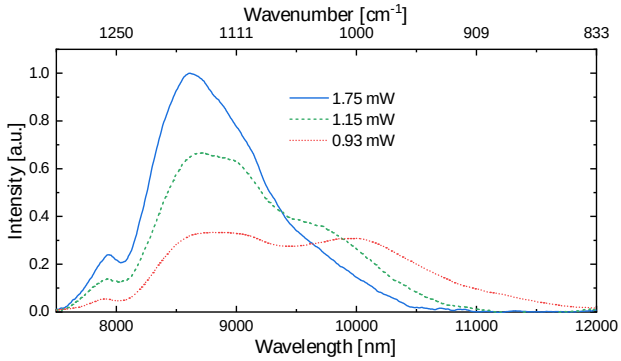

Fig. 2. Optical spectra and corresponding power obtained by DFG, tuning the pump diode current of the optical amplifier that seeds the SC branch. These spectra were measured with a conventional Fourier-transform spectrometer.

out-of-loop phase correction of interferograms (IGMs) [18,19]. This is achieved by tracking, in the near-infrared, relative timing, and carrier phase jitter between the MIR combs with the help of four beat notes that the two driving combs produce with two cw lasers at 1530 and 1565 nm (RIO ORION Laser Source). The beat notes are synchronously digitized with the IGMs by a 200 MS/s card (GaGe Razor Express16XX CompuScope PCIe digitizer board) that provides an upper limit of 100 MHz to the spectral extent of the IGMs. In the post-correction software, the beat note signals are linearly combined to first correct the phase noise in the selected MIR spectral range before resampling on an equidistant time delay grid.

Figure 2 shows spectra of the MIR pulses obtained by DFG by translating the OP-GaP crystal and correspondingly adjusting the supercontinuum generation conditions to maximize the optical power. The overall MIR power (before the beam-splitter) remains around 1 mW in all conditions, even when the idler wavelength is pushed toward 12 µm, and the quantum efficiency is correspondingly reduced. The boundary at 7.5 µm is due to

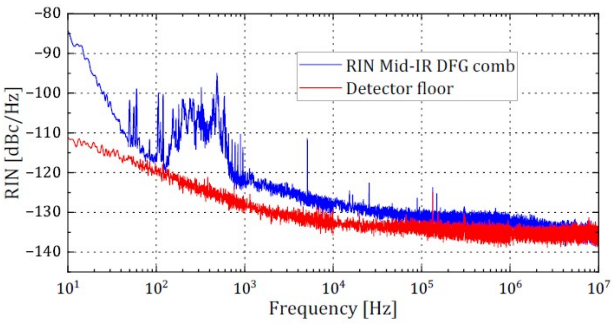

Fig. 3. Relative intensity noise spectrum of the DFG combs measured with a DC-coupled LN-cooled detector with a 40 MHz bandwidth. At high frequencies, the RIN spectrum is limited by the detector noise. This limit is even stronger with the AC-coupled TE-cooled detector used for gas detection.

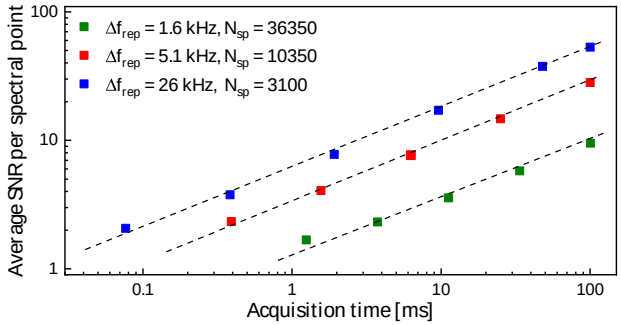

Fig. 4. Average signal-to-noise ratio (SNR) per spectral point as a function of the acquisition time for blank spectra of different spectral width acquired close to the aliasing limit rate.

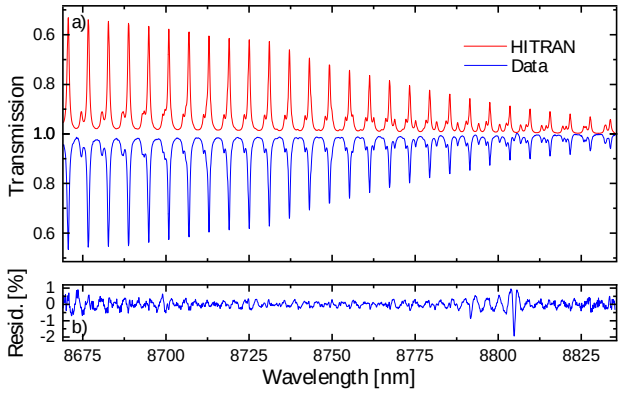

Fig. 5. (a) Experimental N_2O spectra acquired at the conditions of Fig. 4, as compared to HITRAN simulations. Measurement time: 15 s; $\Delta f_{rep} = 26$ kHz (see Supplement 1 for spectra over the entire ν_2 band acquired at $\Delta f_{rep} = 5.1$ kHz). (b) Residuals of Voigt-fitting with respect to total pressure and gas concentration upon cepstral removal of the spectral baseline.

the lack of a suitable poling period in the crystals as the spectral extension of the signal pulses would support the generation of wavelengths down to 7 µm. Figure 3 reports the relative intensity noise (RIN) spectrum of the MIR combs, exhibiting a favorable detector noise-limited plateau of −135 dBc/Hz at the radio frequencies exploited in DCS: this indicates no substantial noise above 1 kHz emerging from the DFG process. Good thermal stability of the oscillators ensured maximum DFG power over minutes with no need to actively control the time delay between the pump and signal pulses. When the delay was intentionally detuned to half the DFG power, the high-frequency part of the RIN spectrum was found to increase by ∼10 dB. An attempt to substitute Raman fibers for the HNLFs led to a much higher and delay-dependent intensity noise on the DFG combs [20], effectively nullifying the advantage of a threefold increase in power offered by Raman fibers [21]. Therefore, we chose HNLF-based DFG combs in this work for dual-comb spectrometry.

Here, DCS was firstly performed without any absorbing medium to characterize the SNR under different optical bandwidth conditions, from 9 THz (7.8–10.2 µm, the full extension of the MIR spectrum), down to 2.5 THz (8.3–8.8 µm, by a bandpass filter) and 0.8 THz (8.65–8.85 µm, by a monochromator). For these bandwidths, the acquisition rate of IGMs was set close to the aliasing limit, at 1.6, 5.1, and 26 kHz, respectively. Figure 4 reports the average SNR achieved per spectral point [22] as a function of the acquisition time up to 100 ms, which is a relatively large time for chemical kinetic studies. All curves follow the squared-root dependence on the acquisition time which is expected when coherent averaging takes place under stationary noise conditions. For a given acquisition time, the higher SNR found for smaller $\Delta\nu$ is due to the lower number of spectral points (N_{sp}). In particular, we achieve a SNR = 2 at the shortest acquisition time of 77 µs considered in the figure, which corresponds to an averaging of two IGMs at $\Delta f_{rep} = 26$ kHz. Accounting for the full number of spectral points, i.e., multiplying SNR by N_{sp}, a figure of merit of $5.2 \cdot 10^5\,\mathrm{Hz}^{0.5}$ is obtained. This is a factor of 10 below the state-of-the-art in the long-wave IR [17] and a factor of 2 below what we obtained at lower Δf_{rep} ($1.1 \cdot 10^6\,\mathrm{Hz}^{0.5}$) where a larger optical power is available, and the detector operates under optimal conditions, just below the onset of nonlinearities [23]. The figure of merit is detector noise-limited in all cases. It is worth pointing out that the SNR values reported in Fig. 4 are obtained at full spectral resolution with spectral points separated by 250 MHz: however, a higher SNR could be obtained by apodizing the interferograms, though at the price of a reduced spectral resolution.

As a demonstration of the developed spectrometer, we chose the ν_2 band of N_2O as it provides intense rovibrational features around 8.7 µm where the power spectral density of the MIR combs is maximum. N_2O was diluted with 90.0% air and housed in a 12 cm long cell at a pressure of 520 mbar. IGMs were acquired at $\Delta f_{rep} = 26$ kHz and averaged over 15 s after the proper phase correction. The computed spectral transmittance of N_2O is shown in Fig. 5(a). It agrees with HITRAN 2020 simulations within 0.5%, to some extent limited by a parasitic etalon, as shown in Fig. 5(b) by the residuals of a Voigt-profile fitting where the relative mole fraction and total pressure were left as free parameters.

The degree of spectral fidelity benefits from a combination of factors, namely high SNR, lack of nonlinearities, efficient phase correction and averaging of IGMs, and accurate baseline retrieval. The latter is a merit of a cepstral approach [24,25] that efficiently separates baseline fluctuations from spectroscopic features. The outlier in the residuals reflects unfitted water lines over a beam propagation path of about 1.5 m. The mole fraction and the pressure retrieved from the fitting are 10.03%

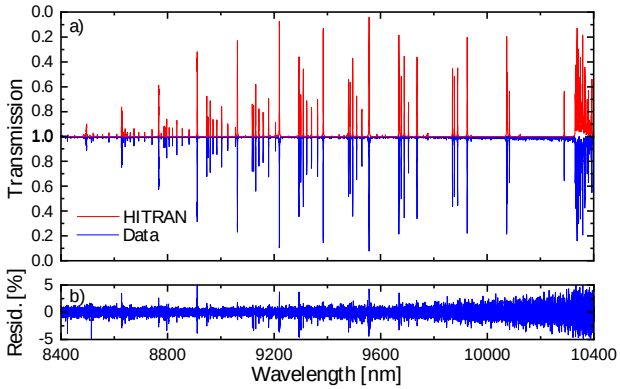

Fig. 6. Same panels of Fig. 5 using an NH_3 sample. Measurement time: 15 s; $\Delta f_{rep} = 1.6$ kHz.

and 526 mbar, respectively, in agreement with the experimental conditions within the uncertainties of our filling procedure.

Additionally, we tested the spectrometer at full bandwidth, over more than 2000 nm (around 9.4 μm), on an ammonia sample diluted at 0.31% in air at a total pressure of 205 mbar. Figure 6 shows the spectrum measured at $\Delta f_{rep} = 1.6$ kHz with an averaging time of 15 s. The concentration and pressure retrieved from the fitting, respectively, equal to 0.33% and 214 mbar, are again in good agreement with the experimental conditions. The larger rms deviation of residuals reflects the lower SNR per spectral point at full bandwidth discussed above. This is more evident at the wings of the spectrum where the power spectral density is lower. In the central part of the spectrum, apart from few spikes that mostly reflect unfitted lines along the free-space path of combs, the residuals remain substantially flat.

In conclusion, we have presented a dual-comb spectrometer based on fiber oscillators and DFG that operates at a fast rate in the water-transparent 7.5–11.5 μm range and that lends itself both for the study of transient phenomena and for environmental monitoring [26]. At $\Delta f_{rep} = 26$ kHz, it exhibits an average SNR per spectral point of 168 $Hz^{0.5}$ which is an order of magnitude higher than the state-of-the-art [17]. Such a high acquisition rate comes together with an effective bandwidth of 0.8 THz and with a reduced optical power at the detector that brings the figure of merit to $5.2 \cdot 10^5$ $Hz^{0.5}$, two times smaller than at lower Δf_{rep} values. Increasing the power spectral density at long wavelengths with large f_{rep} systems remains nontrivial; in the case of the 1 GHz source recently presented in [27], e.g., only 100 μW power was achieved beyond 7 μm compared to 4 mW below 5 μm. A higher power at long wavelengths with high f_{rep} systems thus represents a stimulating challenge for further advancements in the DCS field.

Funding. Clean Combustion Research Center, King Abdullah University of Science and Technology (Competitive Research Grant program, OSR-2019-CRG-4046); HORIZON EUROPE European Innovation Council (EIC-2021-PATHFINDEROPEN-01, 101047137, project "TROPHY").

Disclosures. The authors declare no conflicts of interest.

Data availability. Data underlying the results presented in this paper are available in Ref. [28].

Supplemental document. See Supplement 1 for supporting content.

REFERENCES

1. A. Farooq, A. B. S. Alquaity, M. Raza, *et al.*, Prog. Energy Combust. Sci. **91**, 100997 (2022).
2. S. M. Sarathy, A. Farooq, and G. T. Kalghatgi, Prog. Energy Combust. Sci. **65**, 67 (2018).
3. I. Coddington, N. Newbury, and W. Swann, Optica **3**, 414 (2016).
4. A. Gambetta, R. Ramponi, and M. Marangoni, Opt. Lett. **33**, 2671 (2008).
5. M. Walsh, P. Guay, and J. Genest, APL Photonics **8**, 071302 (2023).
6. G. Villares, A. Hugi, S. Blaser, *et al.*, Nat. Commun. **5**, 5192 (2014).
7. M. Lepère, O. Browet, J. Clément, *et al.*, J. Quant. Spectrosc. Radiat. Transfer **287**, 108239 (2022).
8. G. Millot, S. Pitois, M. Yan, *et al.*, Nat. Photonics **10**, 27 (2016).
9. M. Yan, P.-L. Luo, K. Iwakuni, *et al.*, Light: Sci. Appl. **6**, e17076 (2017).
10. D. A. Long, M. J. Cich, C. Mathurin, *et al.*, Nat. Photonics **18**, 127 (2024).
11. E. Baumann, F. R. Giorgetta, W. C. Swann, *et al.*, Phys. Rev. A **84**, 062513 (2011).
12. G. Ycas, F. R. Giorgetta, E. Baumann, *et al.*, Nat. Photonics **12**, 202 (2018).
13. A. V. Muraviev, V. O. Smolski, Z. E. Loparo, *et al.*, Nat. Photonics **12**, 209 (2018).
14. N. Hoghooghi, P. Chang, S. E. M. Burch, *et al.*, "Complete reactants-to-products observation of a gas-phase chemical reaction with broad, fast mid-infrared frequency combs," arxiv arXiv:2307.07029 (2023).
15. H. Timmers, A. Kowligy, A. Lind, *et al.*, Optica **5**, 727 (2018).
16. A. S. Kowligy, H. Timmers, A. J. Lind, *et al.*, Sci. Adv. **5**, eaaw8794 (2019).
17. S. Vasilyev, A. Muraviev, D. Konnov, *et al.*, Opt. Lett. **48**, 2273 (2023).
18. J. Roy, J.-D. Deschênes, S. Potvin, *et al.*, Opt. Express **20**, 21932 (2012).
19. N. B. Hébert, D. G. Lancaster, V. Michaud-Belleau, *et al.*, Opt. Lett. **43**, 1814 (2018).
20. V. Silva de Oliveira, A. Ruehl, P. Masłowski, *et al.*, Opt. Lett. **45**, 1914 (2020).
21. A. Gambetta, N. Coluccelli, M. Cassinerio, *et al.*, Opt. Lett. **38**, 1155 (2013).
22. P. Guay, M. Walsh, A. Tourigny-Plante, *et al.*, Opt. Express **31**, 4393 (2023).
23. P. Guay, A. Tourigny-Plante, V. Michaud-Belleau, *et al.*, OSA Continuum **4**, 2460 (2021).
24. R. K. Cole, A. S. Makowiecki, N. Hoghooghi, *et al.*, Opt. Express **27**, 37920 (2019).
25. M. Walsh, N. Malarich, F. R. Giorgetta, *et al.*, in *Optica Sensing Congress 2023 (AIS, FTS, HISE, Sensors, ES)* (Optica Publishing Group, 2023), paper JM2B.3.
26. F. R. Giorgetta, J. Peischl, D. I. Herman, *et al.*, Laser Photonics Rev. **15**, 2000583 (2021).
27. N. Hoghooghi, S. Xing, P. Chang, *et al.*, Light: Sci. Appl. **11**, 264 (2022).
28. L. Moretti, M. Walsh, N. Abualsaud, *et al.*, "Fast rate dual-comb spectrometer in the water-transparent 7.5-11.5 μm region," Zenodo: Version 1, 27 February 2024, https://zenodo.org/doi/10.5281/zenodo.10709447.